

## OXIDATION MECHANISMS IN MgO-C REFRACTORIES

Z. Ali Nemati, B. Hashemi and S. K. Sadrnezhad

Dept. of Materials Science and Engineering, Sharif University of Technology, Iran

**Abstract:** Oxidation of graphite in MgO-C refractories can result in degradation of brick properties (By creating porosity and deteriorating the bonding within the structure) and eliminate the effects of graphite in the system and finally shorten the service lifetime of the refractories. Determination of oxidation mechanisms will help to prevent and/or lower the effects of this phenomenon (as a benefit factor in oxidation control).

In this research, the oxidation behavior of MgO-C refractories containing 5–20 wt% graphite, at temperature range from 900°C to 1300°C and in air was studied (based on the weight-loss measurement at regular intervals). For determination of oxidation mechanisms, experimental results were compared with oxidation kinetic equations of a constant dimension body by Shrinkage Core Model. The results indicate that the diffusion through porous layer is the main controlling mechanism of the oxidation process. In the samples with high content of graphite, the gas volume variations due to the CO/CO<sub>2</sub> ratio change may cause the slight shifting of the oxidation mechanism from pure pore diffusion to pore diffusion - external gas transfer mechanism.

### 1. INTRODUCTION

MgO-C Refractories with especial properties were developed not only for new technology of steel making process, but also for consumption reduction of refractories per ton of steel production [1]. One of the main and important problems of MgO- C refractories is oxidation of graphite, especially; at below 1400°C, because, at this temperature range dense layer was not formed and burn out of graphite by air is very fast [2-4]. Graphite oxidation can take place in three mechanisms, which are solid – gas reactions, solid – liquid reactions and solid-solid reactions. In BOF furnaces, refractory can be oxidized with gas during blowing of oxygen, tapping of melt and slag, charging of melt and scrap and at rest time of furnace. In recent years many researches were conducted about parameters affecting oxidation and role of antioxidant in MgO- C refractories [5-8], and different methods were designed for measuring and comparing of oxidation [9-10]. But a few researches based on reassuring of weight loss with time or analysis of gas products had gone to determine kinetic of oxidation [11-15]. Based on researches conducted by X. Li and M. Rigaud [14] (via gas analysis) and N. K. Ghosh et al [15] (via weight loss measuring for a given graphite contact) oxidation equations in one dimension were derived and concluded that Oxidation of graphite is a diffusion control process.

In this research, Oxidation of samples containing 5-20 wt% G at temperature range 900°C-1300°C and in air based on measuring weight loss with time were investigated and the effect of graphite content on oxidation and oxidation mechanism was determined according to shrinking core model (a simple model for gas – solid reactions).

### 2. EXPERIMENTAL PROCEDURE

Cylindrical samples (with 30 mm in diameter and 25 mm height) were prepared using sintered magnesia with a purity of 97% (Table1) and natural china graphite- flakes with an ash content of 5 wt.% and density of 2.26 gr/cm<sup>3</sup> (Table 2). The magnesia grains were in 0-5 mm (at four ranges, 3-5 mm, 2-3 mm, 0.1-2 mm and < 0.1 mm) with size distribution defined by n=0.5 in Andreasen's Equation ( $y=100(d/D)^n$ ). The graphite content of samples was 5-20 wt% and 5 wt% liquid phenolic resin (Novalac, Table 3) was used as binder. Samples were prepared by one direction die press of 120 Mpa. The specimens were tempered at 240°C for 18h and then bulk density and apparent porosity of them measured according to ASTM C-20 in Oil (Table 4).

**Table 1.** Chemical analysis and density of china sintered magnesia

Composition	MgO	CaO	SiO <sub>2</sub>	Al <sub>2</sub> O <sub>3</sub>	Fe <sub>2</sub> O <sub>3</sub>	L.O.I
Percent	97.1	1.26	0.56	0.09	0.89	0.01
Density g/cm <sup>3</sup>	3.51					

**Table 2.** Physical properties of china flake graphite

Properties	%
Carbon	95.17
Moisture	0.02
Volatile material	1.6
Ash	3.3

**Table 3.** Properties of phenolic resin

Properties	Amount	Optimum value
Ph	7.05	8-9
Percent of solid resin	62.6 %	63 – 80 %
Density at 20 C	1.21(gr/cm <sup>3</sup> )	> 1.15
Viscosity	> 10	Min 10
Remained carbon	42.64	> 40 %
Color	No color	No color
Free phenol	1 %	< 1 %

Before oxidation tests, the samples were heated at 600°C for 5 hr in a coke bed to remove the volatile species and to minimize the influence of them. After than, bulk density and apparent porosity of samples remeasured (Table 5). The samples were Oxidized isothermally at temperatures 900°C, 1100°C and 1300°C in a tubular furnace as shown in Fig 1, by natural convection of air. The test sample was placed on an alumina tube and then conducted to the furnace with test temperature. In order to create a unidirectional oxidation process, the bottom and the top surfaces of the sample were covered by a piece of alumina plate to prevent the oxidation from both ends. The weight changes were measured with time at regular intervals and fraction of weight loss was calculated (X) according to below equation:

$$\text{Fraction of weight loss} = X = \frac{\text{Weight loss at time } t}{\text{Total weight loss after complete oxidation}}$$

### 2.1. Shrinking – Core Model (SCM)

The shrinking core model for an isothermal spherical particle (B) which reacts with gas (A) is illustrated in Fig 2 for a particular instant of time, [16]. There is a sharp boundary (the reaction surface) between the no reacted core of solid B and the porous outer shell of solid product (ash layer). The gas film reflected the resistance to mass transfer of gas (A) from the bulk gas to the exterior surface of the particle. As time passes, the reaction surface moves progressively toward the center of the particle. According to the SCM model, three processes involving mass transfer of gas in gas film, diffusion of gas in porous layer and reaction of gas with solid (B) at reaction surface, are rate controlling steps.

According to the cylinder shape of samples, if we consider a thin cylindrical shell in the ash layer at radial position  $r$  and with a thickness of  $dr$  in samples by means of material balance across the shell, the continuity equation for gas (A) will be obtained as below:

**Table 4 .** Bulk density and apparent porosity of samples

Properties	5 wt%G	10 wt%G	15 wt%G	20 wt%G
Bulk density after tempering gr/cm <sup>3</sup>	2.91	2.88	2.86	2.83
Apparent porosity after tempering %	9.55	7.86	6.71	6.28
Bulk density after heating at 600°C gr/cm <sup>3</sup>	2.88	2.85	2.82	2.78
Apparent porosity after heating at 600°C %	13.3	12.10	11.65	11.43

$$\left( \begin{array}{c} \text{rate of input of A} \\ \text{by diffusion at } r+dr \end{array} \right) - \left( \begin{array}{c} \text{rate of output of a} \\ \text{by diffusion at } r \end{array} \right) = \left( \begin{array}{c} \text{rate of accumulation of A} \\ \text{with in the shell} \end{array} \right)$$

$$2\pi r h D_e \frac{\partial c_A}{\partial r} + \frac{\partial}{\partial r} (2\pi r h D_e \frac{\partial c_A}{\partial r}) dr - 2\pi r h D_e \frac{\partial c_A}{\partial r} = \frac{\partial n_a}{\partial t} = \frac{\partial}{\partial t} (2\pi r h d r c_A)$$

$$D_e \left( \frac{\partial^2 c_A}{\partial r^2} + \frac{1}{r} \frac{\partial c_A}{\partial r} \right) = \frac{\partial c_a}{\partial t} \tag{1}$$

If we assume that the concentration gradient for gas through the ash layer is established rapidly relative to movement of the reaction surface, we may treat the diffusion as steady-state diffusion for a fixed value of  $r$ , then Eq. 1 becomes

$$\frac{d^2 c_A}{dr^2} + \frac{1}{r} \frac{dc_A}{dr} = 0 \tag{2}$$

This assumption is called the quasi-steady-state approximation (QSSA) and is valid because of the great difference in densities of gas and solid. By solving the above equation according to boundary condition [16] results in

$$t = \frac{\rho_B R}{bc_{Ag}} \left\{ \frac{X_B}{2K_{Ag}} + \frac{R}{4D_e} [X + (1 - X_B) \ln(1 - X_B)] + \frac{1}{k_{AS}} \left[ 1 - (1 - X_B)^{\frac{1}{2}} \right] \right\} \tag{3}$$

This equation is the summation of three mechanisms that are gas layer mass transfer control, ash layer diffusion control and surface reaction rate control, and may be one mechanism (one process) dominates to others. Then if we draw each terms verses time, a liner relation will indicate that which term or process controls the overall system behavior.

### 3. RESULTS AND DISCUSSION

The fraction of weight loss  $X$  versus time for different temperatures 900°C, 1100°C and 1300° C at constant graphite contents 10 wt% and 20 wt% are shown in Figs. 3-4. It is obvious that the rate of weight loss was very fast in the beginning of oxidation and decreases gradually because of increasing the thick-

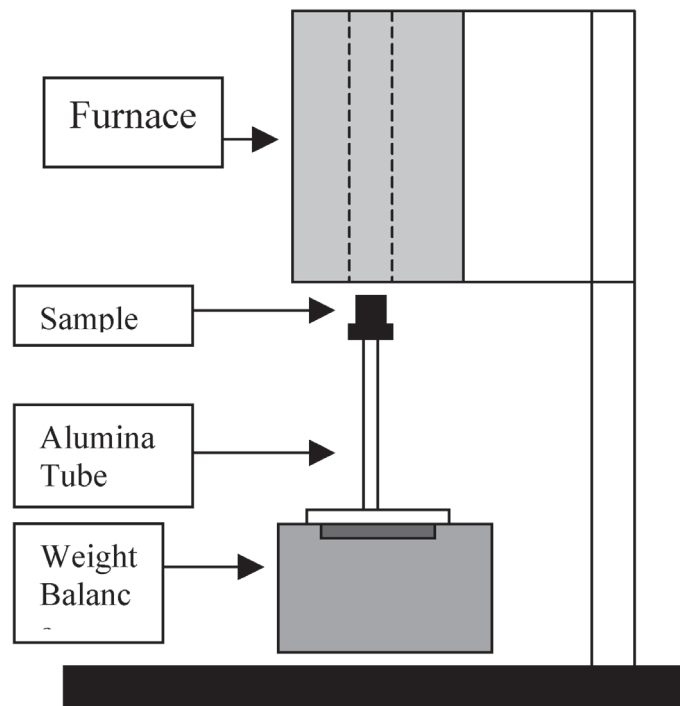


Fig. 1. Schematic view of setup, used for weight loss measuring.

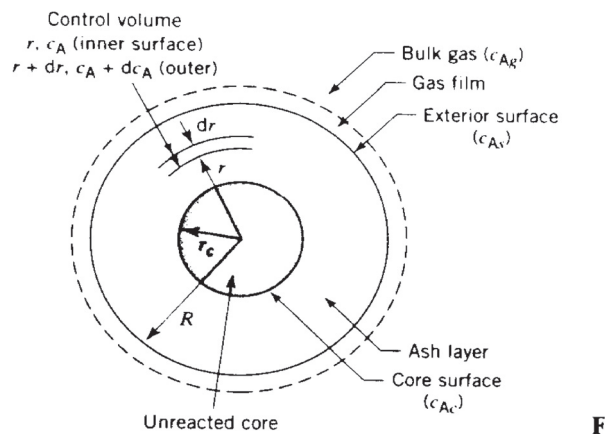


Fig. 2. The shrinking core model for an isothermal spherical particle

ness of oxidized layer. The rate of weight loss increased with temperature. These observations indicate a diffusional behavior, which represents faster transfer of oxygen at the higher temperatures with lower oxidation rates at the greater weight loss. Increase of chemical reactivity of the graphite is another reason for increasing of weight loss with temperature.

The fraction of weight loss with time and with 5%, 10%, 15% and 20% graphite at isothermal temperatures 900°C, 1100°C and 1300°C are shown in Figs. 5–7. By increasing the graphite content, the weight loss decreases and at 15wt% and 20wt%G weight losses were almost same. At higher graphite contents, more graphite existed per unit volume of the sample. A higher amount of O<sub>2</sub> must, therefore, diffuse into the sample to oxidize the higher C content. Although the diffusion rate increases (due to the increase of porosity of oxidized layer with graphite content and weight loss increases), however, because of changing of the produced gas composition, this increase is not proportional to the graphite content of the sample and the fractional weight loss decreases by the amount of graphite, as shown in the figures.

Cross section of samples with 10wt% graphite after oxidation at different temperatures is shown in Fig. 8. It is seen that the oxidation of graphite is topochemical in nature and reaction surface is sharp, then we can

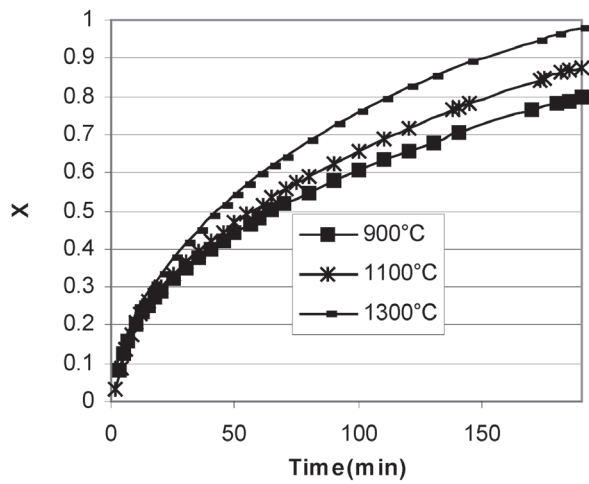


Fig. 3. Fractional weight loss of samples 10wt%G at different temperatures

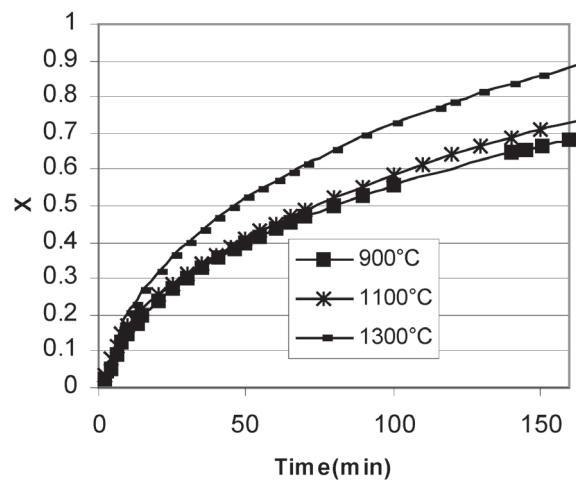


Fig. 4. Fractional weight loss of samples 20wt%G at different temperatures

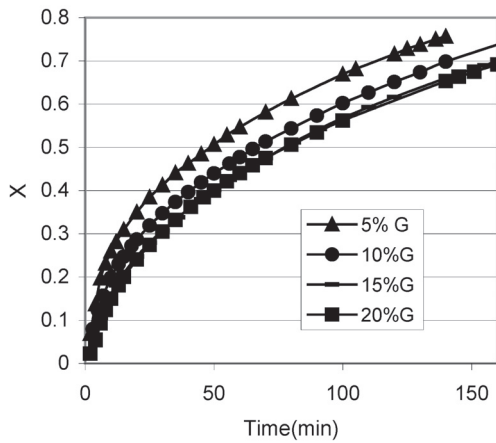


Fig. 5. Fractional weight loss of samples containing various amount of graphite at 900°C

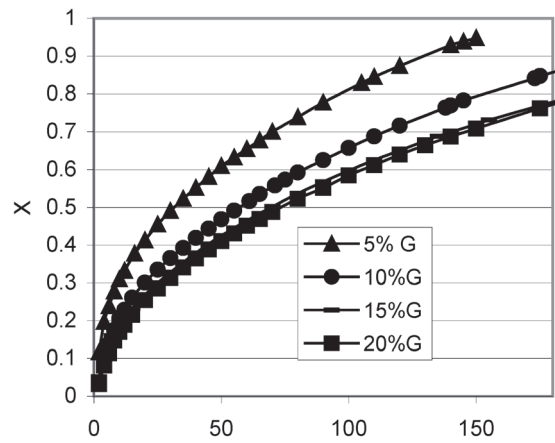


Fig. 6. Fractional weight loss of samples containing various amount of graphite at 1100°C

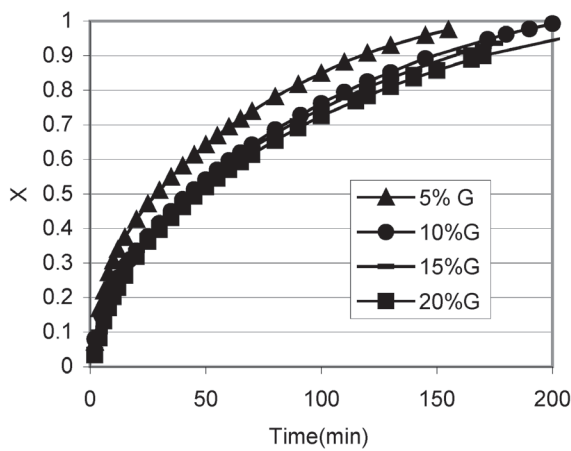


Fig. 7. Fractional weight loss of samples containing various amount of graphite at 1300°C

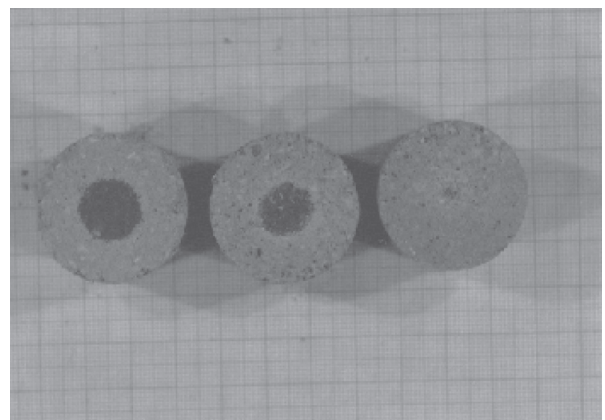


Fig. 8. Cross section of samples containing 10wt%G, Oxidized at different temperatures (from left to right 900°C, 1100°C and 1300°C)

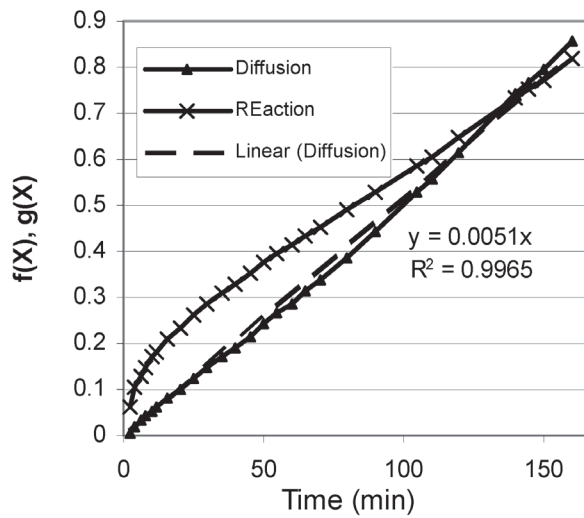


Fig. 9.  $f(X)$  and  $g(X)$  versus time of sample with 5% graphite at 1300° C

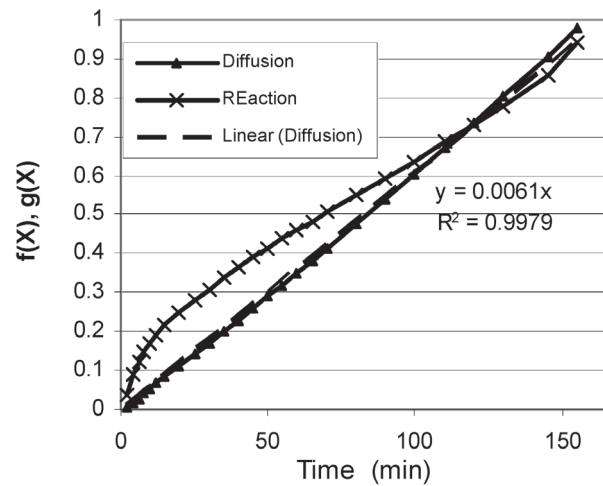


Fig. 10.  $f(X)$  and  $g(X)$  versus time of sample with 5% graphite at 1100° C

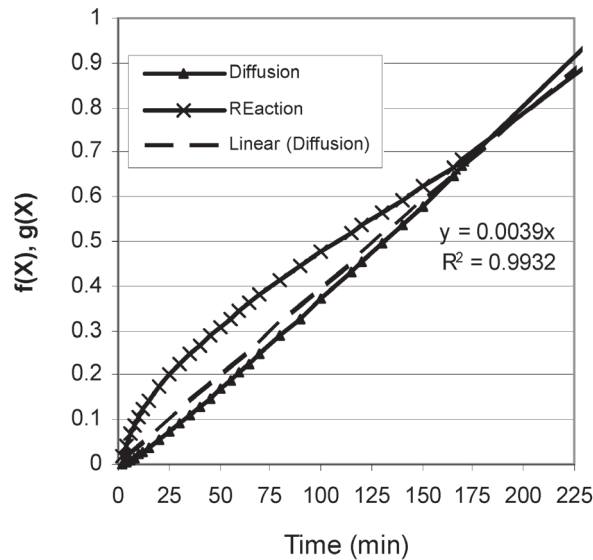


Fig. 11.  $f(X)$  and  $g(X)$  versus time of sample with 20% graphite at 1300° C

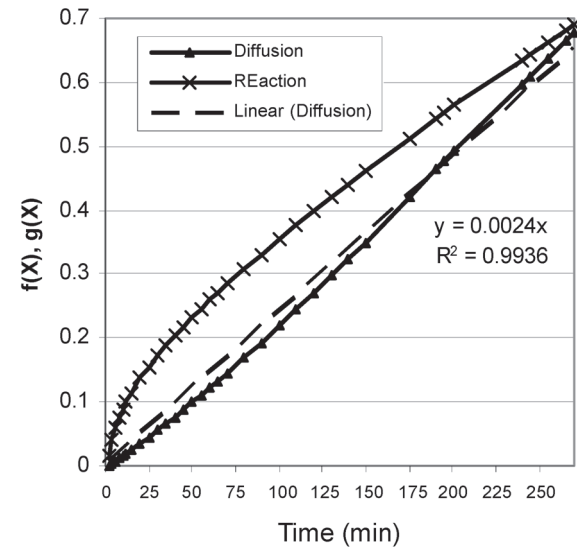


Fig. 12.  $f(X)$  and  $g(X)$  versus time of sample with 20% graphite at 1100° C

relate the decarburized layer thickness with fractional weight loss ( $X=1-(r_c/R)^2$ ).

The variation of  $f(X)$  and  $g(X)$  versus time, (Where  $f(X)$  is  $X+(1-X)\ln(1-X)$  for diffusion mechanism and  $g(X)$  is  $1-(1-X)^{0.5}$  for chemical reaction mechanism) were shown in Figs. 9 – 12. As it is clear that relation between diffusion term and time is relatively linear in comparison to chemical reaction term (Gas layer mechanism does not compare with others because if the gas layer mechanism would be dominating, a linear relation must exist between  $X$  and time but Figs 5-7, do not show such behavior). But with increasing of graphite content and temperature, deviation from linearity increases. At the samples containing higher percentage of graphite, the oxidation mechanism tends to slightly deviate from pure pore diffusion control. The gas volume variations due to the  $CO/CO_2$  ratio change may cause the slight shifting of the oxidation mechanism from pure pore diffusion to pore diffusion - external gas transfer mechanism.

#### 4. CONCLUSION

1. Oxidation increases exponentially with temperature because diffusion of oxygen and reaction of



- graphite with oxygen increase when temperature increases.
2. With increasing of the graphite content, the rate of weight loss increases due to the formation of a more porous oxidized layer, but the fractional weight loss decreases due to the increase of the initial carbon content. The weight loss increase is not, however, proportional to the enhancement of the graphite content. This may be attributed to the combined influences of the reaction front area change, CO/CO<sub>2</sub> ratio change and inter diffusion coefficients variations.
  3. Oxidation mechanism is pore diffusion, which means the diffusion of oxygen through decarburized layer is processes control.
  4. When graphite content of the samples increases, the oxidation mechanism tends to slightly deviate from pure pore diffusion control. The gas volume variations due to the CO/CO<sub>2</sub> ratio change may cause the slight shifting of the oxidation mechanism from pure pore diffusion to pore diffusion - external gas transfer mechanism.

## REFERENCES

1. S. Banerjee, Recent developments in steel – making refractories, Unitecr 2002, p.1033.
2. A. Yamaguchi, Control of oxidation-redaction in MgO-C refractories, Taikabutsu overseas, Vol.4, No.1, p.32.
3. R.E. Moore, et.al, Reactions between magnesia-graphite-metal components of B.O.F type refractories: Role of impurities, Unitecr 91, p.165.
4. A. Watanabe, H. Takahashi, Mechanism of dense magnesia layer formation near the surface of MgO-C brick, J.Am.Ceram.Soc, 69[9] c-213-214 (1986).
5. A. Yamaguchi, H. Tanaka, Role and behavior of non-oxide compounds added to carbon – containing refractories, Unitecr 91, p.19.
6. K. Ichikawa, et.al, Suppression effects of aluminum on oxidation of MgO-C bricks, Taikabutsu overseas, Vol.15, No.2, p.21.
7. I. Tsuchiya, S. Tanaka, Effect of metallic additives on oxidation-reduction reaction in MgO-C bricks under vacuum at elevated temperature, Unitecr 95, p.156.
8. A. Yamaguchi, S. Zhang, Behavior of antioxidants added to carbon containing refractories, Unitecr 95, p.341.
9. Li Xiang-min, M. Rigaud, Methods of characterize oxidation resistance for magnesia-carbon refractories, Chinas Refractories, Vol.5, No.3, p.13, 1996.
10. D.J. Griffin, et.al, Consideration for the measurement and improvement of oxidation resistance in dolomite-carbon and magnesia-carbon refractories, Unitecr 91, p.253.
11. A. Wolfert, et.al, Thermo-gravimetric studies of magnesia-carbon reactions, Unitecr 91, p.256.
12. L. Rontgi, et.al, Kinetics of reduction of magnesia with carbon, Thermochemica Acta, 390, (2002), 145-151.
13. G. Routschka, The oxidation of carbon –contaning refractories, Unitecr 2001, p.2.
14. X. Li, et.al, Oxidation kinetics of graphite in magnesia-carbon refractories, J.Am.Ceram.Soc, 78[4] 965-71 (1995).
15. N.K. Ghosh, et.al, Oxidation mechanism of MgO-C in air at various temperature, British Ceramic Transactions, Vol.99, No.3, p.124, 2000.
16. R.W. Missen, C.A. Mims, Introduction to chemical reaction engineering and kinetics, John Wiley & Sons, Inc, p.224, 1999.